

Humidity sensing properties of ZnO colloid crystals coated on quartz crystal microbalance by the self-assembly method

Juan Xie^{a,b,*}, Hu Wang^{a,**}, Yuanhua Lin^b, Ying Zhou^b, Yuanpeng Wu^b

^aState Key Laboratory of Oil and Gas Reservoir Geology and Exploitation, Southwest Petroleum University (SWPU), Chengdu 610500, China

^bCollege of Materials Science and Engineering, Southwest Petroleum University, Chengdu 610500, China

Received 29 August 2012; received in revised form 10 October 2012; accepted 11 October 2012

Available online 22 October 2012

Abstract

ZnO colloid crystals were coated on quartz crystal microbalance (QCM) by the self-assembly method. Field emission scanning electron microscopy and X-ray diffraction were used to analyze the morphology and crystal structure of ZnO colloid crystals. The sensing behavior was examined by measuring the resonance frequency shifts of QCM. The device exhibits excellent humidity sensing properties in the whole humidity range from 11% to 95%, such as good linearity, fast response time and recovery time, excellent reliability, and long-term stability. We also discussed the adsorption and desorption of water molecules on ZnO colloid crystals at different humidity conditions.

Crown Copyright © 2012 Published by Elsevier Ltd and Techna Group S.r.l. All rights reserved.

Keywords: D. ZnO; Colloid crystal; Humidity sensing; Quartz crystal microbalance (QCM)

1. Introduction

Accurate and reliable measurement of humidity has become an important issue in various fields, such as automobile industry, semiconductor manufacturing, pharmaceutical industry, soil moisture monitoring, packaging, and food processing [1–3].

Several promising sensing techniques including field effect transistors (FET) [4], bulk acoustic wave (BAW) [5], surface acoustic wave (SAW) [6] and quartz crystal microbalance (QCM) [7–11] have been developed and applied to enhance the accuracy of humidity sensors. Among above various sensing technologies, the QCM is an extremely sensitive and powerful tool for monitoring mass changes in the nanogram scale. The mass change (Δm) on surface of the quartz crystal is calculated

by using the Sauerbrey equation from the frequency change (Δf) [12]:

$$\Delta f = -\frac{2f_0^2}{A\sqrt{\mu\rho}} \times \Delta m = -C \times \Delta m$$

where f_0 is the resonance frequency of the fundamental mode of the QCM crystal, A is the area of the gold disk coated onto the crystal, μ is the shear modulus of quartz, and ρ is the density of the crystal. The frequency shift is directly proportional to the adsorbed mass on the QCM with sensitive coating materials. Therefore, the use of QCM coated with sensitive materials has become an alternative approach for detecting low humidity. Many kinds of sensing materials were prepared on QCM wafer to detect humidity, including organic polymers, metal oxides, and porous inorganic/organic materials [13–20]. However, limit to our knowledge, no reports on QCM-based sensors with coating ZnO colloid crystals have been reported.

In this work, ZnO colloid crystals were fabricated by a self-assembly method on a QCM wafer as the humidity sensor. The morphology and crystal structure of ZnO colloid crystals were analyzed by emission scanning

*Corresponding author at: State Key Laboratory of Oil and Gas Reservoir Geology and Exploitation, Southwest Petroleum University (SWPU), Chengdu 610500, China. Tel./fax: +86 28 83037346.

**Corresponding author. Tel./fax: +86 28 83037346.

E-mail addresses: Jennyx99@126.com (J. Xie), Senty78@126.com (H. Wang).

electron microscopy and X-ray diffraction, respectively. Humidity sensing capabilities of the ZnO colloid crystals were investigated by QCM technique at room temperature by varying the relative humidity (RH) from 11% to 95%.

2. Experimental

2.1. Fabrication of ZnO colloid crystals on QCM

ZnO colloid crystals were synthesized by the self-assembly method. 0.01 mol Zinc acetate dihydrate was added into 100 ml diethylene glycol. This reaction solution was heated under 180 °C. After reaching the working temperature, precipitation of ZnO spheres occurred. The intermediate product was placed in a centrifuge. The polydisperse powder was discarded and the supernatant was used in the next step. A secondary reaction was then performed to produce the monodisperse ZnO spheres, which began in the same way as the primary reaction. Prior to reaching the working temperature, however, typically at 170 °C, some volume of the primary reaction supernatant was added into the solution. After reaching 180 °C, the reaction was stirred for several hours. When the heat source was removed, flask cooled to room temperature. The ZnO colloidal suspension was prepared and the size of the spheres varied inversely and monotonically with the amount of primary supernatant added.

The suspension was dropped onto the QCM wafers. Then the coatings were dried in a furnace at 80 °C for 1 h. After evaporating the organic solvent, the white films formed on the surface of the QCM wafers.

2.2. Measurements

The morphology of the ZnO films on the QCM was observed with the field emission scanning electron microscope (FESEM, JSM-7500F). The crystal structure of ZnO colloid crystals was characterized by X-ray diffraction (XRD, BEDE-DI, with Cu-K α radiation, $\lambda = 1.542 \text{ \AA}$). The controlled humidity environments were achieved with saturation aqueous solutions of LiCl, MgCl₂, Mg(NO₃)₂, NaCl, KCl, and KNO₃ in a closed glass vessel at room temperature, which yielded 11%, 33%, 55%, 75%, 85%, and 95% RH, respectively [21]. Each of the saturated salt solution was kept in the glass chamber for 24 h before the measurement. The sensing properties of the sensors to humidity were examined by measuring the resonance frequency shifts of QCM because of the additional mass loading. The resonance frequencies were measured by a QCM digital controller (QCM200, Stanford Research Systems). The QCM sensors were suspended above a half-filled closed container without contacting the solution and they were stored in a dry environment after the test runs. The frequency signals were measured during the adsorption process (RH from 11% to other RH %) and desorption process (RH from other RH % to 11%).

3. Results and discussion

3.1. Materials characterization

The FESEM image in Fig. 1 indicates that the average diameter of the colloid spheres is about 450 nm. It can be observed at the same time that the colloid sphere is composed of primary particles. Fig. 2 shows the XRD pattern of the as-prepared colloid crystals. All the diffraction peaks can be indexed as the hexagonal phase ZnO reported in the standard card (JCPDS 36-1451). No obvious characteristic peaks are observed for other impurities.

3.2. Humidity sensing property

Fig. 3 describes the frequency shift (left) and the dependence of the frequency shifts of the sensor (right)

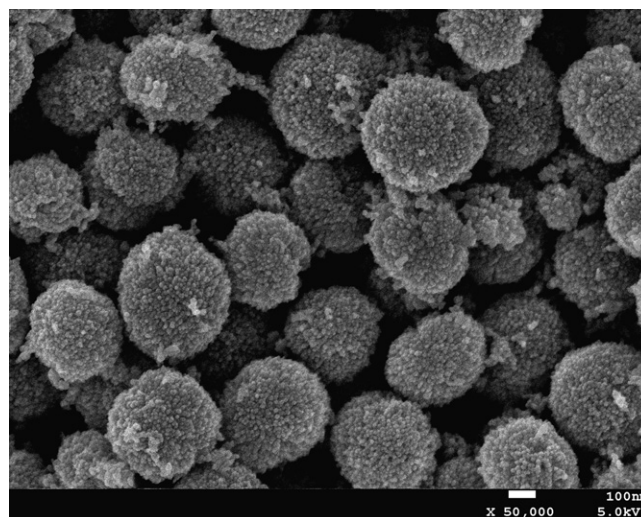


Fig. 1. Typical FESEM images of ZnO colloid crystals.

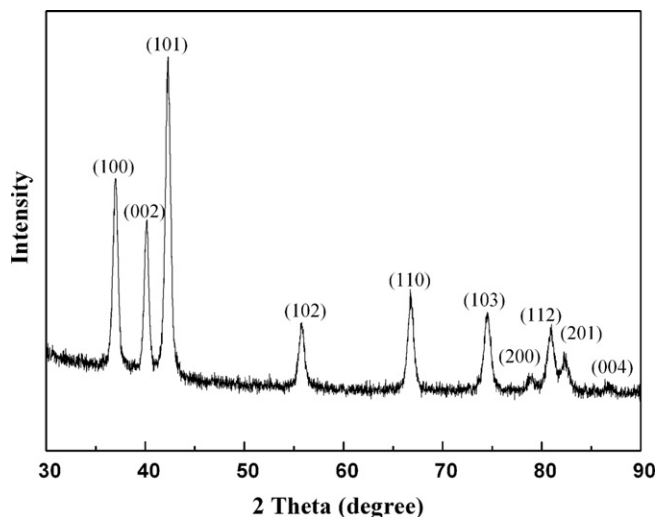


Fig. 2. XRD spectra of ZnO colloid crystals.

as a function of RH (between 11% and 95% RH). As can be seen from the figure, the resonant frequency shifts increase with an increase of RH. The results indicate that the frequency of the sensor shifts remarkably. It can be seen in Fig. 3 that the frequency shifts as a function of the RH do not indicate a linear tendency with increasing RH. However, the frequency shifts followed a logarithmic demonstrate good linear log (Δf) toward RH in the range from 11% to 95% and the coefficient of determination, R^2 , was 0.9947.

It is well known that response and recovery behavior is an important characteristic for evaluating the performance of the sensing materials. The humidity response and recovery characteristic curves at RH conditions between 11% and 95% are given in Fig. 4. The response time is defined as the time taken for 90% of the sensor response change after an increase in the stimulus is accomplished. The recovery time is the time needed for 90% of the sensor response change after stimulus removal is accomplished [22]. In a humidity sensor, the response and recovery time correspond to the adsorption and desorption of water molecules on the surface of sensing materials. The two

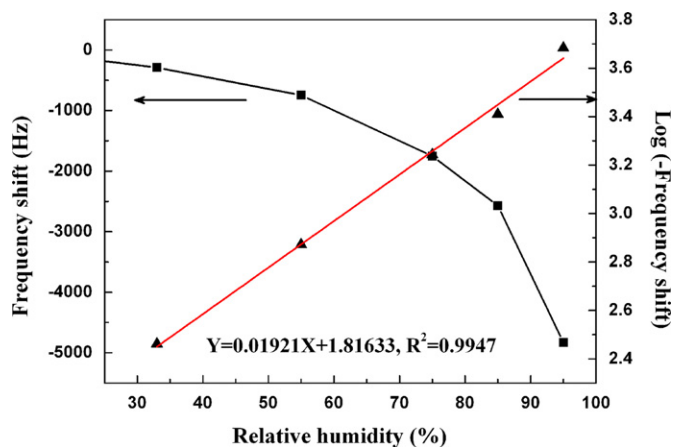


Fig. 3. Frequency shifts of QCM humidity sensor (left), the dependence of the frequency shifts of sensor (right).

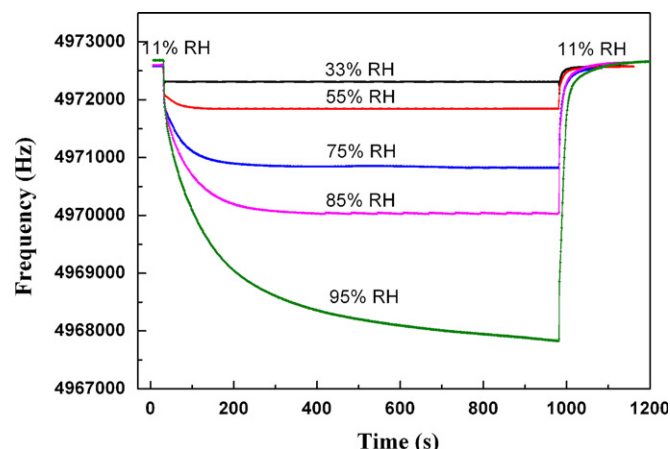


Fig. 4. Response and recovery curve of QCM sensors.

parameters are determined by alternatively exposing the sensing materials to solutions the lowest and the highest RH values. The response time was about 2.8 s, 13.2 s, 58 s, 105 s and 152.2 s, and the recovery time was about 24 s, 15.4 s, 11.7 s, 11 s and 10 s, respectively. The results show fast response and recovery processes. It can be observed that the response time increased with increasing RH. It can be also seen that the recovery time decreased with increasing RH. The results imply that at the low RH (33% and 55%) the recovery time is longer than response time. However, at the high RH (75%, 85%, and 95%), it exhibits shorter recovery time than response time. It is attributed to the nanoscale primary particles formed on the colloid crystal surface, which make the H_2O molecules move through the materials easily, resulting in a rapid recovery speed at high RH.

Hysteresis is the time lag in the adsorption and desorption processes, and is usually used to estimate to reliability of a humidity sensor. According to Fig. 5, the adsorption/desorption RH hysteresis curves of the sensor were measured in the humidity range from 11% to 95%. The maximum humidity hysteresis is around 2.0% RH in 85% RH for these sensors. It is obvious that the sensor exhibits a narrow hysteresis loop during the cyclic humidity operation. This indicates a good reliability of the obtained sensors.

It is manifested from Fig. 6 that the sensor displays outstanding long-term stability at different RH. The measurement was repeated at room temperature every 5 days. Slight variation in frequency shift was observed over the time period, indicating that the sensor has prominent long-term stable characteristic.

3.3. Humidity sensing mechanism

The adsorbed water model base on physical and chemical actions can be used to explain the response to humidity of ZnO colloid crystals. The ZnO colloid crystals can establish an adsorption–desorption equilibrium under the

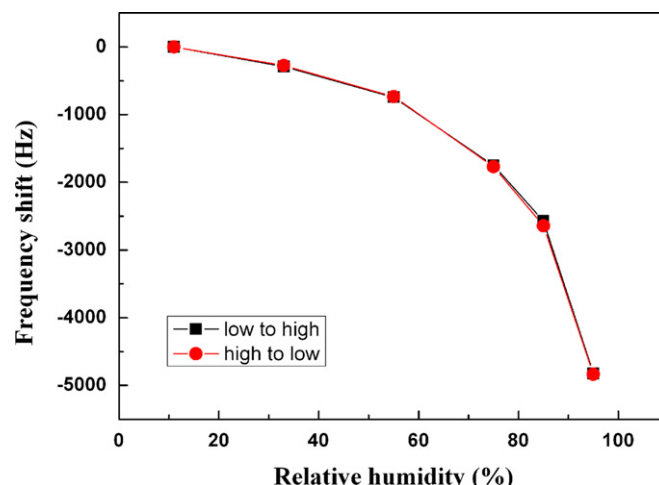


Fig. 5. Hysteresis of QCM humidity sensor.

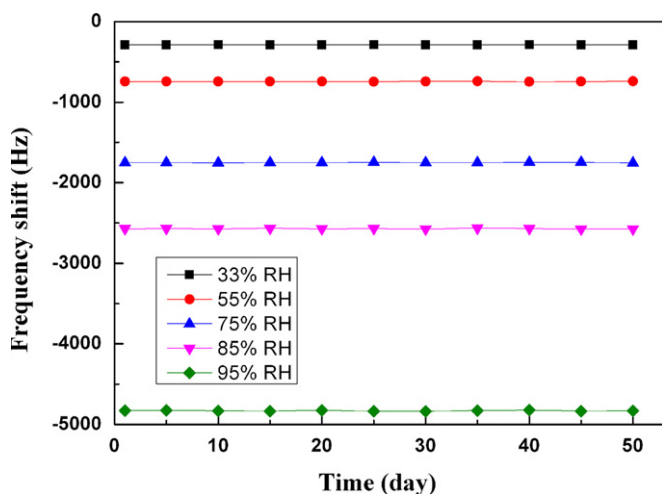


Fig. 6. Stability of ZnO colloid crystals coated QCM wafer after exposure in air for 50 days.

actions of Van Der Waals force and hydrogen bond in a certain humidity environment. The humidity environment changes will cause equilibrium shift, indicating a change of resonance frequency of the QCM caused by the change of mass. When the QCM is placed in a lower RH than environment humidity, the water molecules will desorb to air atmosphere from the surface of the sensing film, resulting in a resonance frequency increase due to decrease of mass on the beam of QCM. On the contrary, when the QCM appears in a higher relative humidity than environment humidity, the water molecules will adsorb on the surface of the film to reach a new equilibrium. When the mass on the QCM increases, the resonance frequency decreases [3]. High response contributes to big specific surface area of ZnO colloid crystals allowing water molecules to reach more active sites from the surfaces.

There are two adsorption processes. First of all, water molecules are chemisorbed on active sites of the ZnO colloid spheres by forming the hydroxyl ions. With increase in humidity, water molecules are physisorbed onto this hydroxyl layer by attaching with two neighboring hydroxyl groups through hydrogen double bonds [23]. On the other hand, the chemisorptions–desorption equilibrium time is longer than the physisorption–desorption equilibrium time. Therefore, under the low water vapor condition, the recovery time is longer than response time. On the contrary, under the high water vapor condition, the recovery time is shorter than response time.

4. Conclusion

In conclusion, highly sensitive humidity QCM sensors coated with ZnO colloid crystals have been fabricated. The results describe that with the increase of humidity values, the adsorption of water molecules will increase. Under the low water vapor condition, the recovery time is longer than response time. Under the high water vapor condition, the recovery time is shorter than response time. The sensors

have good sensing characteristics in the range from 11% to 95% RH, such as good linearity, fast response/recovery time, excellent reliability, and long-term stability.

Acknowledgments

This work was financially supported by the Fundamental Research Funds of Southwest Petroleum University (no. 2012XJZ017) and Sichuan College Laboratory of Materials of Oil and Gas Field (no. 12YQT016).

References

- [1] H. Jamil, S.S. Batool, Z. Imran, M. Usman, M.A. Rafiq, M. Willander, M.M. Hassan, Electrospun titanium dioxide nanofiber humidity sensors with high sensitivity, *Ceramic International* 38 (2012) 2437–2441.
- [2] M.Y. Su, J. Wang, Y.W. Hao, Development of Y^{3+} and Mg^{2+} -doped zirconia thick film humidity sensors, *Materials Chemistry and Physics* 126 (2011) 31–35.
- [3] Y.H. Zhu, H. Yuan, J.Q. Xu, P.C. Xu, Q.Y. Pan, Highly stable and sensitive humidity sensors based on quartz crystal microbalance coated with hexagonal lamelliform monodisperse mesoporous silica SBA-15 thin film, *Sensors and Actuators B* 144 (2010) 164–169.
- [4] A. Star, R.R. Han, V. Joshi, J.R. Stetter, Sensing with Nafion coated carbon nanotube field-effect transistors, *Electroanalysis* 16 (2004) 108–112.
- [5] H. Seh, T. Hyodo, H.L. Tuller, Bulk acoustic wave resonator as a sensing platform for NO_x at high temperatures, *Sensors and Actuators B* 108 (2005) 547–552.
- [6] M. Penza, G. Cassano, Relative humidity sensing by PVA-coated dual resonator SAW oscillator, *Sensors and Actuators B* 68 (2000) 300–306.
- [7] Y.L. Sun, Y.Z. Chen, R.J. Wu, M. Chavali, Y.C. Huang, P.G. Su, C.C. Lin, Poly(L-lactide) stabilized gold nanoparticles based QCM sensor for low humidity detection, *Sensors and Actuators B* 126 (2007) 441–446.
- [8] Y.L. Sun, R.J. Wu, Y.C. Huang, P.G. Su, M. Chavali, Y.Z. Chen, C.C. Lin, In situ prepared polypyrrole for low humidity QCM sensor and related theoretical calculation, *Talanta* 73 (2007) 857–861.
- [9] P.G. Su, Y.L. Sun, C.C. Lin, Novel low humidity sensor made of TiO_2 nanowires/poly(2-acrylamido-2-methylpropane sulfonate) composite material film combined with quartz crystal microbalance, *Talanta* 69 (2006) 946–951.
- [10] Y.S. Zhang, K. Yu, R.L. Xu, D.S. Jiang, L.Q. Luo, Z.Q. Zhu, Quartz crystal microbalance coated with carbon nanotube films used as humidity sensor, *Sensors and Actuators B* 120 (2005) 142–146.
- [11] W.L. Hu, S.Y. Zhou, L.T. Liu, B. Ding, H.P. Wang, Highly stable and sensitive humidity sensors based on quartz crystal microbalance coated with bacterial cellulose membrane, *Sensors and Actuators B* 159 (2011) 301–306.
- [12] G. Sauerbrey, The use of quartz oscillators for weighing thin layers and for microweighing, *Zeitschrift für Physik* 155 (1959) 206–222.
- [13] C.Y. Lee, G.B. Lee, Micromachine-based humidity sensors with integrated temperature sensors for signal drift compensation, *Journal of Micromechanics and Microengineering* 13 (2003) 620–627.
- [14] P.G. Su, Y.L. Sun, C.C. Lin, Humidity sensor based on PMMA simultaneously doped with two different salts, *Sensors and Actuators B* 113 (2006) 883–886.
- [15] H.W. chen, R.J. Wu, K.H. Chan, Y.L. Sun, P.G. Su, The application of CNT/Nafion composite material to low humidity sensing measurement, *Sensors and Actuators B* 104 (2005) 80–84.
- [16] A. Erol, S. Okur, N. Yagmurcukardes, M.C. Arikian, Humidity-sensing properties of a ZnO nanowire film as measured with a QCM, *Sensors and Actuators B* 152 (2011) 115–120.

- [17] P.G. Su, Y.P. Chang, Low-humidity sensor based on a quartz-crystal microbalance coated with polypyrrole/Ag/TiO₂ nanoparticles composite thin films, *Sensors and Actuators B* 129 (2008) 915–920.
- [18] S. Okur, M. Kus, F. Ozel, M. Yilmaz, Humidity adsorption kinetics of water soluble calyx[4]arene derivatives measured using QCM technique, *Sensors and Actuators B* 145 (2010) 93–97.
- [19] J. Wang, K. Shi, Study of polymer humidity sensor array on silicon wafer, *Journal of Materials Science* 39 (2004) 3155–3157.
- [20] G.C. Miceli, M. Yang, Y. Li, N. Camaioni, A. Martelli, A. Zanelli, Effect of the doping level on the conductance of polymer-salts complexes in the presence of humidity, *Sensors and Actuators B* 97 (2004) 362–368.
- [21] W.W. Zhang, R.W. Wang, Q. Zhang, J.X. Li, Humidity sensitive properties of K-doped mesoporous silica SBA-15, *Journal of Physics and Chemistry of Solids* 73 (2012) 517–522.
- [22] P.K. Kannan, R. Saraswathi, J.B. Rayappan, A highly sensitive humidity sensor based on DC reactive magnetron sputtered zinc oxide thin film, *Sensors and Actuators B* 164 (2010) 8–14.
- [23] L.L. Gu, K.B. Zheng, Y. Zhou, J. Li, X.L. Mo, G.R. Patzke, G.R. Chen, Humidity sensors based on ZnO/TiO₂ core/shell nanorod arrays with enhanced sensitivity, *Sensors and Actuators B* 159 (2011) 1–7.